Received: 31 March 2020 | Revised: 18 July 2020 | Accepted: 23 August 2020

DOI: 10.1002/jsp2.1124

SPECIAL ISSUE ARTICLE

JOR Spine OPEN ACCESS

Age-related molecular changes in the lumbar dorsal root ganglia of mice: Signs of sensitization, and inflammatory response

Kathleen Vincent[1,2] | Chethana Prabodhanie Gallage Dona[1,3] | Todd J Albert[3,4] | Chitra Lekha Dahia[1,2]

[1]Orthopedic Soft Tissue Research Program, Hospital for Special Surgery, New York, New York

[2]Department of Cell and Developmental Biology, Weill Cornell Medicine, Graduate School of Medical Science, New York, New York

[3]Department of Medicine, Weill Cornell Medical College, New York, New York

[4]Orthopaedic Surgery, Hospital for Special Surgery, New York, New York

Correspondence
Chitra Lekha Dahia, Assistant Professor, Weill Cornell Medical College, Assistant Scientist, Hospital for Special Surgery, 515 East 71st Street, New York, NY 10021, USA.
Email: dahiac@hss.edu

Funding information
National Institute of Arthritis and Musculoskeletal and Skin Diseases, Grant/Award Number: R01AR065530; S & L Marx Foundation; Starr Foundation; Gerstner Family Foundation; National Institutes of Health

Abstract

Aging is a major risk factor for numerous painful, inflammatory, and degenerative diseases including disc degeneration. A better understanding of how the somatosensory nervous system adapts to the changing physiology of the aging body will be of great significance for our expanding aging population. Previously, we reported that chronological aging of mouse lumbar discs is pathological and associated with behavioral changes related to pain. It is established that with age and degeneration the lumbar discs become inflammatory and innervated. Here we analyze the aging lumbar dorsal root ganglia (DRGs) and spinal cord dorsal horn (SCDH) in mice between 3 and 24 months of age for age-related somatosensory adaptations. We observe that as mice age there are signs of peripheral sensitization, and response to inflammation at the molecular and cellular level in the DRGs. From 12 months onwards the mRNA expression of vasodilator and neurotransmitter, *Calca* (CGRP); stress (and survival) marker, *Atf3*; and neurotrophic factor, *Bdnf*, increases linearly with age in the DRGs. Further, while the mRNA expression of neuropeptide, *Tac1*, precursor of Substance P, did not change at the transcriptional level, TAC1 protein expression increased in 24-month-old DRGs. Additionally, elevated expression of NFκB subunits, *Nfkb1* and *Rela*, but not inflammatory mediators, *Tnf*, *Il6*, *Il1b*, *or Cox2*, in the DRGs suggest peripheral nerves are responding to inflammation, but do not increase the expression of inflammatory mediators at the transcriptional level. These results identify a progressive, age-related shift in the molecular profile of the mouse somatosensory nervous system and implicates nociceptive sensitization and inflammatory response.

KEYWORDS

aging, allodynia, disc degeneration, dorsal root ganglia, inflammation, nerve injury, peripheral sensitization

1 | INTRODUCTION

Chronic pain is a disease, which disproportionately affects the elderly.[1] In part, this is due to their elevated risk of inflammatory and degenerative diseases, such as, disc degeneration and arthritis, which develop into intractably painful conditions. Projections from the 2017 US census bureau estimate the number of people over the age of 65 will nearly double by 2060, making it the fastest growing age demographic in the United States.[2] The importance of this aging demographic has not gone unnoticed in the pain field. Research efforts at the intersection of age and pain has outpaced researched efforts performed exclusively on pain over the past 30 years, and has emerged as a subfield.[3] There are multiple pathological processes contributing to an altered nociceptive state with age. Peripheral nerve damage and demyelination,[4,5] supraspinal pain circuitry dysregulation,[6] increased circulating inflammatory mediators,[7,8] and innervation of degenerating joints[9,10] are all potential conditions leading to chronic pain in the elderly. Therefore, as the aging body is a unique physiological environment, preclinical models need to accurately reflect the aging condition to obtain clinically relevant data.

To better address the challenges of understanding age-related disorders, physiologically aging mouse model systems are invaluable. Aged mice exist in a distinctive pro-inflammatory physiological milieu, which responds uniquely to trauma[11-14]; and much like in humans, aged mice display behavioral patterns consistent with ongoing pain.[15,16] Previously, we reported that age significantly predicts increasing axial discomfort and hind-paw cold allodynia in male and female mice.[15] Our previous studies have further demonstrated pathological degenerative changes in the lumbar discs—a common phenomenon in aging humans in aging mice,[15,17,18] including innervation and vascularization.[15] Currently, whether and how degenerative changes in the disc affect sensory nerves and their modulation of nociception is unknown.

To assess the consequences of degenerative changes with aging on nociceptive signaling, we characterize the lumbar dorsal root ganglia (DRGs) and the lumbar spinal cord dorsal horn (SCDH) using mice as a model system. To this end, we selected markers to analyze sensitization, inflammation, nerve growth, temperature sensation, and stress response in the DRGs and SCDH of mice (shown in Figure 1). We look for signs of nociceptive sensitization using the neuropeptides, Calcitonin gene-related peptide alpha (CALCA, or CGRP) and tachykinin 1 (TAC1, or substance P). Additionally, as inflammation is central to the aging process, we investigate the peripheral nerves for both production of and response to pro-inflammatory mediators. We also examine the regulation of neurotrophic factor, nerve growth factor (NGF), and its receptor, TRKA, in the DRGs. We assess the contribution of peripheral nerves in regulating sensitivity toward hot and cold stimuli by measuring TRPA1, a cold-sensing ion channel, and TRPV1, a heat-sensing ion channel. Finally, neuropeptide Y (NPY) and activating transcription factor 3 (ATF3) are used to identify cell stress.[19-21] We chose to specifically investigate the lumbar 4 (L4), L5, and L6 DRGs and lumbar SCDH because of its particular relevance to age-related disc degeneration and

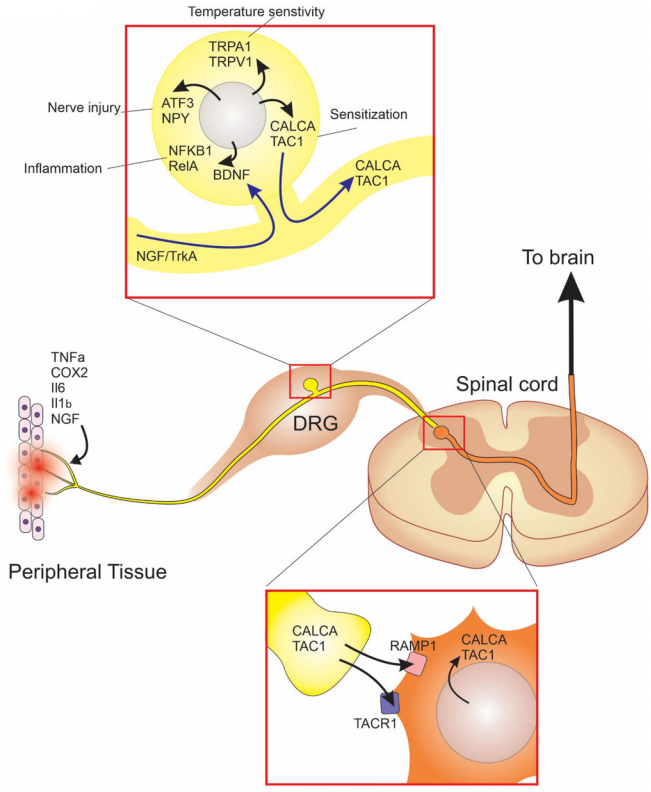

FIGURE 1 Signaling pathways of interest in the peripheral and central nociceptive pathway. Tissues innervated by the DRGs release proinflammatory mediators and neurotrophic factors, which act on their receptors on nerve endings and stimulate the NFκB response in DRGs. Damage to axons through compression or injury in age-related degenerative diseases including intervertebral disc degeneration stimulates the expression of nerve injury markers and cell stress, such as, ATF3 and NPY. In response to damage or inflammation DRGs can dynamically regulate expression of cold and heat sensing ion channels, TRPA1 and TRPV1, and nociceptive neuropeptides, CALCA and TAC1. Nociceptive neuropeptides are released into the dorsal horn in the spinal cord where they act on their receptors RAMP1 and TACR1 to regulate expression in spinal nociceptive neurons

associated neurological symptoms. Previously we reported that the lumbosacral discs show the most severe pathologies with age,[15,18] with a significant increase observed in histopathological scores by 18 months.[18] Additionally, the L4-6 DRGs in mice contain the majority of the nerves that comprise the sciatic nerve, which is often the target for painful radiculopathy. Overall, this study provides a description of the changes in the sensory system in aging mice as it relates to the chronification of pain and implications of disc degeneration.

2 | MATERIALS AND METHODS

2.1 | Mice

All mice were maintained in accordance with the National Institutes of Health Guide for the Care and Use of Laboratory Animals, and all

experiments were carried out in accordance with institutional guidelines under Institutional Animal Care and Use Committee (IACUC) approved at Weill Cornell Medical College (WCMC). Male and female mice between the ages of 3 to 24 months of age and based on a C57BL/J6, FVB, or mixed background were used in the study. Both male and female mice are maintained in the same animal facility with a 12:12 dark: light cycle with food (PicoLab Rodent Diet 20; 25% protein, 13% fat, 62% carbohydrates) available ad libitum. Males and females are housed in separate cages with 2-5 animals per cage. Cages include autoclaved Aspen chips (WF Fisher & Sons) bedding and enrichment in the form of nesting material (EnviroPak, WF Fisher & Sons). The use of mixed strains in our data improves generalizability of experimental results.

Experiments used between four to eight mice per age cohort, with a mix of females and males per cohort. For qPCR studies, originally five animals per cohort were used; for the markers that showed a significant main effect of age by one-way ANOVA, qPCR assays were independently replicated with an additional three samples per cohort. The time points chosen for data collection were informed by our previously study showing immunofluorescent changes in the DRGs at 3 months (comparable to 20-30 years in humans[22]), 12 months (comparable to 38-47 years in humans[22]), and 24 months (comparable to 56-69 years in humans[22]). These ages were again chosen for histology; however, as the data revealed that between three to 12 months there are no changes in protein expression or in behavioral repertoire,[15] we focused qPCR and Western blot data on 12, 18, and 24 month old animals in order to better capture the aging progression past middle-age. The number of male and female mice in each assay is in Table 1.

2.2 | Tissue collection for histology

To collect DRGs and spinal cord for histology, animals were sacrificed by CO_2 and their lumbar spines grossly dissected and placed in ice-cold 4% paraformaldehyde (PFA, Sigma, 158 127) prepared in 1x phosphate buffered saline (PBS) for 2 hours to firm the soft tissue for dissection. A laminectomy was performed as described previously[23] to expose the spinal cord and the lumbar region was identified by the lumbar enlargement. A 1 cm region of the lumbar spinal cord dorsal horn and the L4, L5, and L6 DRGs were extracted and fixed in buffered 4% PFA for an additional 4 hours at 4°C. The tissues were washed in PBS 3×10 minutes and processed through increasing gradients of buffered sucrose in 10%, 20%, and 30% concentrations, and containing 0.01% sodium azide (Sigma, S2002) at 4°C. The DRGs and

TABLE 1 Number of male (#M) and female (#F) mice used per assay in each cohort

			3 months		12 months		18 months		24 months		Total	
Assay	Tissue	Gene	#M	#F	#M	#F	#M	#F	#M	#F	#M	#F
qPCR	DRG	*Calca*	N/A	N/A	3	5	4	4	3	5	10	14
qPCR	SCDH	*Calca*	N/A	N/A	2	3	2	3	3	2	7	8
qPCR	SCDH	*Ramp1*	N/A	N/A	2	3	2	3	3	2	7	8
qPCR	DRG	*Tac1*	N/A	N/A	2	3	2	3	3	2	7	8
qPCR	SCDH	*Tac1*	N/A	N/A	2	3	2	3	3	2	7	8
qPCR	SCDH	*Tacr1*	N/A	N/A	2	3	2	3	3	2	7	8
qPCR	DRG	*Trpa1*	N/A	N/A	3	5	4	4	3	5	10	14
qPCR	DRG	*Nfkb1*	N/A	N/A	3	5	4	4	3	5	10	14
qPCR	DRG	*Rela*	N/A	N/A	3	5	4	4	3	5	10	14
qPCR	DRG	*Il1b*	N/A	N/A	2	3	2	3	3	2	7	8
qPCR	DRG	*Il6*	N/A	N/A	2	3	2	3	3	2	7	8
qPCR	DRG	*Tnf*	N/A	N/A	2	3	2	3	3	2	7	8
qPCR	DRG	*Gfap*	N/A	N/A	2	3	2	3	3	2	7	8
qPCR	DRG	*Cox*	N/A	N/A	2	3	2	3	3	2	7	8
qPCR	DRG	*Atf3*	N/A	N/A	3	5	4	4	3	5	10	14
qPCR	DRG	*Npy*	N/A	N/A	3	5	4	4	3	5	10	14
qPCR	DRG	*Bdnf*	N/A	N/A	3	5	4	4	3	5	10	14
IF	DRG	CALCA	3	2	2	3	N/A	N/A	3	2	8	7
IF	DRG	TRPV1	3	2	2	3	N/A	N/A	3	2	8	7
IF	DRG	NGF	3	2	2	3	N/A	N/A	3	2	8	7
IF	DRG	TRKA	3	2	2	3	N/A	N/A	3	2	8	7
WB	DRG	TAC1	N/A	N/A	1	3	1	3	1	3	3	9

Abbreviations: IF, immunofluorescence; N/A, not application; qPCR, quantitative polymerase chain reaction; WB, Western blot.

TABLE 2 List of molecular markers and TaqMan probes used for their analysis

Category	Gene name	Gene symbol	Assay ID	Function
Inflammation	nuclear factor of kappa light polypeptide gene enhancer in B cells 1, p105/p50	*Nfkb1*	Mm00476361_m1	NFKB subunit activated in response to inflammation, produces the p50 and p105 subunits[66]
	v-rel reticuloendotheliosis viral oncogene homolog A, p65	*Rela*	Mm00501346_m1	NFKB subunit activated in response to inflammation, produces the p65 subunit[67,68]
	Glial fibrillary acidic protein	*Gfap*	Mm01253033_m1	Marker of glial activation in response to inflammation[69]
	Interleukin 6	*Il6*	Mm00446190_m1	Secreted in acute phase of inflammation, important for the transition to chronic inflammation and pain[70]
	Interleukin 1 beta	*Il1b*	Mm00434228_m1	Increased bilaterally in DRGs following peripheral inflammation[71]
	Tumor necrosis factor	*Tnf*	Mm00443258_m1	Inflammatory mediator, induces ectopic discharge in c-fibers[72]
	Cytochrome oxidase subunit 2 (COX2)	*Cox2*	Mm03294838_g1	Inflammatory mediator, produced in spinal cord and DRGs following inflammation[73,74]
Nociception	Calcitonin Related Polypeptide Alpha	*Calca*	Mm00801463_g1	Nociceptive neuropeptide involved in the transmission of and sensitization to noxious stimuli from PNS to CNS[34,75]
	Tachykinin Precursor 1	*Tac1*	Mm01160362_m1	TAC1 protein is a nociceptive neuropeptide involved in the transmission of noxious stimuli from PNS to CNS[76,77]
	Receptor Activity Modifying Protein 1	*Ramp1*	Mm00489796_m1	Receptor that allows CALCA to bind to the calcitonin-receptor-like receptor in the SCDH[78,79]
	Tachykinin Receptor 1	*Tacr1*	Mm00436892_m1	Receptor in spinal cord that binds TAC1 to transmit nociceptive input in chronic pain conditions[80]
	Transient Receptor Potential Cation Channel Subfamily A Member 1	*Trpa1*	Mm01227437_m1	Cold sensing ion channel involved in cold sensitivity in both inflammation and nerve injury[81]
Nerve Injury	Neuropeptide Y	*Npy*	Mm01410146_m1	Neuropeptide induced following nerve injury[82] increases firing rates of DRGs[83]
	Activating Transcription Factor 3	*Atf3*	Mm00476033_m1	Transcription factor induced following nerve injury[21]
Neurotrophic factors	Brain Derived Neurotrophic Factor	*Bdnf*	Mm04230607_s1	Expression in DRGs contributes to chronic pain[84]
Internal Control	Glyceraldehyde-3-Phosphate Dehydrogenase	*Gapdh*	Mm99999915_g1	Stable housekeeping gene in the DRGs[25]

spinal cord were incubated for 8 to 12 hours at 4°C with each sucrose concentration to cryoprotect and embed the tissue. The DRGs and spinal cord were then molded in Tissue-Tek optimum cutting temperature (O.C.T., VWR, 102094-106) and stored at −80°C until sectioned. Cryosections of the DRG were collected at 8 μm thickness in the coronal plane and sections of the spinal cord were collected at 8 μm thickness in the transverse plane using a Leica cryostat (Leica Biosystems, CM3050S).

2.3 | Tissue collection for RNA

Following dissection, the lumbar SCDH was placed in RNA*later* (Invitrogen, AM7021) overnight at 4°C. The L4, L5, and L6 DRGs were dissected from the spine and the nerve roots and nerve fibers excised proximal to the DRGs. All three pairs of the DRGs were placed in RNA*later* overnight at 4°C. The RNA*later* was removed the next day and the samples snap frozen and stored at −80°C.

TABLE 3 List of primary and secondary antibodies used for immunofluorescence analysis

Primary antibody	Company	Catalogue #	Concentration (mg/ml)	Dilution	Secondary antibody
rabbit anti-CALCA	Abclonal	A5542	3.68	1:100	Alexa Fluor© 647-AffiniPure donkey anti-rabbit, 1:200, Jackson ImmunoResearch Laboratories, 711-605-152
rabbit anti-NTRK1	Abclonal	A2098	1.72	1:100	same as above
rabbit anti-NGF	BosterBio	m00341	1.00	1:100	same as above
rabbit anti-TRPV1	Abclonal	A8564	4.19	1:100	same as above

2.4 | RNA extraction and qPCR analysis

RNA isolation was performed using the QIAzol (Qiagen, 79 306) and RNeasy Micro Kit (Qiagen, 74 004). Frozen DRG and SCDH samples were lysed in QIAzol and homogenized using a sterilized Omni Tissue Homogenizer (OMNI International, THP115). Samples were centrifuged at 12 000 RPM for 12 minutes at 4°C, supernatant collected and incubated an additional 5 minutes at room temperature. Chloroform (Sigma, C2432) was added at one fifth the volume and incubated for 10 minutes at room temperature. The sample was then centrifuged for 15 minutes at 4°C. The aqueous phase was collected and an equal volume of RNase-free 70% ethanol (Pharmaco, 111 000 200) was added and transferred to the Qiagen spin columns. The RNA purification protocol provided by the RNeasy Micro Kit was followed and RNA was eluted with warm (75°C) 15 µl of RNase-free water. RNA concentration was assessed using a NanoDrop One (ThermoFisher).

Immediately following RNA isolation, cDNA synthesis was performed using the SuperScript IV first-strand synthesis system using manufacturer's protocol (ThermoFisher Scientific, 18 091 050) in a C1000 touch thermal cycler (Bio-Rad, 1 851 148). The resulting cDNA was diluted to 2 ng/µl using RNase-free water and stored at −20°C.

Table 2 lists the TaqMan probes used for qPCR analysis. Exon-spanning gene-specific TaqMan probes were obtained from ThermoFisher Scientific. All probes were conjugated to FAM-MGB except of the internal control *Gapdh*, which was conjugated to VIC-MGB. qPCR reactions were run in duplicate using 8 ng of cDNA with TaqMan Multiplex Master Mix (ThermoFisher, 4 461 881) in a CFX96 Real Time System (Bio-Rad, 1 855 196). Relative expression was determined and values are expressed as $2^{-[Ct(\text{target gene})-Ct(Gapdh)]}$. GAPDH is used as an internal control in aging mouse data,[24] and has been validated as a reliable internal control in models of nerve injury.[25] The average Ct value of *Gapdh* in our experiments is also reported in Table 4.

2.5 | Immunofluorescent staining and analysis

Immunostaining was performed as previously described.[26] Cryosections were air-dried and rehydrated in PBS. Cryosections were permeabilized with either PBS containing 0.1% Triton-X (0.1% PBST) (for CALCA and TRPV1) or 10 mM sodium citrate (for NTRK1 and NGF) for 20 minutes and at room temperature. Sections were blocked using 10% normal donkey serum (Jackson ImmunoResearch, 017-000-121) with 4% IgG-free BSA (Jackson ImmunoResearch, 001-000-162) in 0.1% PBST for 1 hour at room temperature in a humidified chamber. Cryosections were incubated with primary antibodies (listed in Table 3) overnight at 4°C in a humidified chamber. Slides were then washed 3×10 minutes with 0.1% PBST to remove unbound antibody and then incubated with the Alexa Fluor conjugated secondary antibody (listed in Table 3) for 1 hour at room temperature. Negative control samples were incubated only with the Alexa Fluor conjugated secondary antibodies. Secondary antibody was washed 3×10 minutes with 0.1% PBST and incubated for 10 minutes with 1:5000 DAPI (Life Technologies, D1306) in PBS to counterstain nuclei, with a final wash in PBS for 10 minutes and mounted with ProLong Gold Antifade mounting media (ThermoFisher, P10144). Samples were imaged together within a week of staining and stored at 4°C. Negative control sections were used to establish appropriate microscope laser and exposure settings before images the experimental samples.

The sections were imaged using DAPI and Cy5 filter cubes of the Nikon Eclipse wide-field microscope and NIS Elements AR software (Nikon, Japan). Images were captured at 20× magnifications. Mean fluorescent intensity (MFI) analyses and cell size distribution of DRGs were carried out using the region of interest (ROI) tool in the NIS Elements AR software. Measurements were performed by outlining 50 cells for each serial section of the DRG with three biological replicates by a researcher blind to the experimental condition, yielding 150 cells per DRG level per animal. Change in protein expression was assessed by taking the median of the 150 MFI values for both the L4 and L5 levels and comparing across cohorts. To visualize which DRGs (small, medium, or large) express the protein of interest, the diameter of each outlined cell was calculated from the cell area as follows: $=2\times\sqrt{\frac{cell\ area}{\pi}}$. Cells were considered to be positive for a protein of interest if their MFI was greater than the average MFI of all the cells for that protein. Histograms showing the proportion of positive cells at each size were generated by taking the number of positive cells at a given diameter divided by the total number of cells sampled. To ensure there was no bias in cell selection between cohorts, the distribution of cell sizes was compared across conditions and found to be indistinguishable (Figure 2B). Thus, differences reported in cell size distribution histograms are not attributable to differences in the number of small, medium, and large cells sampled.

TABLE 4 Relative gene expression in L4-6 DRGs and lumbar SCDH from mice at specified age. *P*-values are based on Dunnett's post-hoc test. Raw Ct value of *Gapdh* included in last column

			Relative gene expression to *Gapdh* (S.E.M)n = 5–8 per cohort						*P*-value	
	Tissue	Gene	12 months		18 months		24 months		12 vs 24	18 vs 24
Nociception	DRG	*Calca*	0.549	(0.083)	0.952	(0.189)	1.067	(0.207)	0.0747	0.8455
	SCDH	*Calca*	0.071	(0.009)	0.104	(0.022)	0.163	(0.0388)	0.0543	0.2410
	SCDH	*Ramp1*	0.033	(6.51×10^{-3})	0.065	(3.52×10^{-2})	0.091	(3.22×10^{-2})	0.2796	0.7445
	DRG	*Tac1*	3.05×10^{-4}	(1.22×10^{-4})	8.43×10^{-4}	(3.22×10^{-4})	5.61×10^{-4}	(4.31×10^{-4})	0.7883	0.4855
	SCDH	*Tac1*	4.96×10^{-3}	(1.48×10^{-3})	$6.\times10^{-3}$	(8.15×10^{-3})	8.15×10^{-3}	(2.74×10^{-3})	0.6308	0.8107
	SCDH	*Tacr1*	9.30×10^{-3}	(4.71×10^{-3})	7.06×10^{-3}	(2.75×10^{-3})	4.55×10^{-3}	(2.85×10^{-3})	0.5561	0.8387
Cold	DRG	*Trpa1*	0.012	(2.31×10^{-2})	0.025	(7.26×10^{-2})	0.026	(4.87×10^{-2})	0.1037	0.9590
Inflammation	DRG	*Nfkb1*	3.03×10^{-3}	($\times10^{-3}$)	3.99×10^{-3}	(5.70×10^{-4})	8.31×10^{-3}	(9.21×10^{-4})	**0.0002**	**0.0016**
	DRG	*Rela*	0.030	(3.33×10^{-3})	0.048	(7.80×10^{-3})	0.059	(0.010)	**0.0239**	0.4908
	DRG	*Il1b*	1.21×10^{-3}	(4.80×10^{-4})	5.95×10^{-4}	(1.38×10^{-4})	1.31×10^{-3}	(1.78×10^{-4})	0.9997	0.5542
	DRG	*Il6*	5.79×10^{-5}	(1.72×10^{-5})	4.81×10^{-5}	(2.10×10^{-5})	1.03×10^{-4}	(3.73×10^{-5})	0.2117	0.0636
	DRG	*Tnf*	2.29×10^{-10}	(4.75×10^{-11})	4.74×10^{-10}	(1.65×10^{-10})	2.05×10^{-10}	(1.95×10^{-11})	0.9755	0.2230
	DRG	*Gfap*	5.01×10^{-3}	(1.03×10^{-3})	7.90×10^{-3}	(4.17×10^{-4})	5.24×10^{-3}	(1.59×10^{-3})	0.9899	0.3401
	DRG	*Cox*	1.52	(0.178)	2.24	(0.307)	1.67	(0.185)	0.8906	0.5123
Nerve injury	DRG	*Atf3*	2.11×10^{-3}	(4.84×10^{-4})	3.81×10^{-3}	(7.23×10^{-4})	5.99×10^{-3}	(8.23×10^{-4})	**0.0030**	0.0835
	DRG	*Npy*	3.81×10^{-4}	(1.19×10^{-4})	8.95×10^{-4}	(2.67×10^{-4})	8.10×10^{-3}	(9.13×10^{-5})	0.0567	0.8661
Nerve growth	DRG	*Bdnf*	5.18×10^{-4}	(1.05×10^{-4})	9.14×10^{-4}	(1.98×10^{-4})	1.20×10^{-3}	(2.35×10^{-4})	**0.0437**	0.4948
Ct of *Gapdh*	DRG	*Gapdh*	23.47	(0.4380)	23.47	(0.5712)	23.25	(0.5931)	0.9999	0.9999

2.6 | Western blot

L4-6 DRGs were collected in whole and placed in 50 µl of RIPA buffer (Sigma, R0278) containing protease inhibitors (cOmplete ULTRA tablet mini EDTA-free EASYpack, Roche, 05-892-791-001) and phosphatase inhibitors (PhosSTOP, Roche, 04-906-845-001) at concentrations specified by the manufacturer. Tissue was initially lysed with mechanical disruption using DNase, RNase free microtube and pestle (Argos, P9950-901) on ice. Tissue was then sonicated using the Bioruptor Pico sonication device (Diagenode, B01060010) in 2 cycles, each cycle consisting of a 30 second "on" phase and 30 second "off" phase at 4°C. Samples were centrifuged at 14 000 RPM for 20 minutes at 4°C and the supernatant transferred and stored at −20°C. Protein concentration was determined by Bradford assay using the Bio-Rad Protein Assay Dye Reagent Concentrate (BioRad, 5 000 006) and the Ultraspec 2100 Pro photometer (Harvard Bioscience, 2100). 30 micrograms of protein was resolved by 12.5% SDS-PAGE and transferred onto nitrocellulose membrane using a Trans-blot semi-dry (Bio-Rad, 1 703 940) apparatus. Membranes were blocked in 5% non-fat milk in Tris-buffered saline (TBS, Corning, 46-012-CM) with 0.1% Tween 20 (Sigma, P1379) (TBS-T) for 1 hour at room temperature and with constant agitation. Blots were cut and probed with rat anti-TAC1 (1:500, abcam, ab7340) or mouse anti-alpha-tubulin (Sigma, T9026, 1:2000) in blocking buffer and incubated overnight at 4°C on a rocker. Blots were washed 3×10 minutes in TBS-T and probed with peroxide-conjugated secondary antibody, either Peroxidase-AffiniPure goat anti-rat IgG H + L (Jackson ImmunoResearch Laboratories, 111-035-144) or Peroxidase-AffiniPure goat anti-mouse IgG H + L (Jackson ImmunoResearch Laboratories, 115-035-003) at a 1:2000 dilution in blocking buffer. Blots were washed 3×10 minutes in TBS-T and exposed to enhanced chemiluminescent substrate Pierce ECL Western (ThermoFisher, 32 209) prior to imaging using the ChemiDoc Touch Imaging System (Bio Rad, 1 708 370). Blots were quantified using ImageJ freeware gel analysis tools taking the area under the curve as a measure of band intensity. TAC1 band intensity was normalized to the intensity of the alpha-tubulin band. Alpha-tubulin was selected as internal control as its expression is not affected by peripheral inflammation or injury.[27,28]

2.7 | Statistical analysis

All statistics were carried out using either the GraphPad Prism 8 or the SPSS version 24 softwares. qPCR data were analyzed by both simple linear regression comparing age and expression level normalized to *Gapdh* and one-way ANOVA comparing with Dunnett's post-hoc comparison between 24 months and all other ages using GraphPad Prism 8. DRG immunofluorescence data were analyzed using a two-way ANOVA with DRG level being a repeated factor and age being the between factor using GrapPad Prism 8. Western blot data were analyzed using a one-way ANOVA comparing TAC1 band intensity normalized by alpha-Tubulin intensity between three age groups. Dunnett's post-hoc comparison was used to compare 24-month-old samples to three and 12-month-old samples for all immunofluorescence and Western blot data using GrapPad Prism 8. All one-way ANOVA data were tested for homogeneity of variance using the Brown-Forsythe test; those that failed the assumption were instead evaluated using the non-parametric Kruskal-Wallis test. For each analysis, one data point refers to sample collected from one biological replicate.

3 | RESULTS

3.1 | Expression of peripheral and central sensitization markers increases with age

Previously it was reported that the distribution of small-, medium-, and large-diameter DRGs does not change with age.[29] First, we determined the distribution of cell sizes in DRGs with age in our experiment and confirmed that it remains constant in mice throughout their adult lifespan (Figure 2A,B). The constant distribution of small, medium and large DRGs with age indicate that there is no change in the proportion of nociceptive afferents with advanced age, and changes in nociceptive signaling must arise from the properties of these nociceptors.

To better understand the properties of the nociceptors, we used immunofluorescence analysis to assess the protein expression and distribution of CALCA, a neuropeptide and a vasodilator produced by nociceptors and released during the relay of nociceptive signaling (Figure 2C). Immunofluorescence analysis revealed that the MFI of CALCA protein within individual L4 and L5 DRG neurons was significantly impacted by age (^{2,22} F = 7.986, *P* = .0025, n = 5 per age cohort) (Figure 2D). Post-hoc tests revealed that CALCA protein expression in the L4 DRGs is significantly greater by 24 months compared with both 3 months (^{22} t = 2.449, *P* = .0421) and 12 months (^{22} t = 2.603, *P* = .0302) old mice. In the L5 DRGs, CALCA protein expression at 24 months was significantly greater than at 12 months (^{22} t = 2.571, *P* = .0324). Next, we determined the proportion of CALCA-expressing cells by measuring L4 and L5 cell size in each age cohort (Figure 2E). As previously reported,[30] and regardless of age, we observed cells staining positively for CALCA protein are predominantly small to medium diameter neurons (Figure 2E). In 24-month-old mice, CALCA protein expression is greater in the small-diameter neurons. To assess whether CALCA protein is transcriptionally regulated, we performed qPCR analysis for *Calca* mRNA on the L4-6 DRGs in mice between 10 and 24 months of age (Figure 2F). All qPCR data were normalized to *Gapdh* which did not significantly differ between the age groups (^{2,21} F = 0.2665, *P* = .7686, n = 8 per cohort)(Table 4), making it an appropriate house-keeping gene for qPCR. Linear regression shows that from 10 months onwards there is a linear increase in *Calca* mRNA indicating age is a significant predictor of *Calca* mRNA expression (^{1,22} F = 4.570, r^2 = 0.1720, *P* = .04736, n = 24). Despite this, the overall increase in *Calca* mRNA expression is minimal, as 24-month-old mice do not have an appreciably greater relative expression of *Calca* mRNA to *Gapdh* mRNA than 12-month-old mice (Table 4).

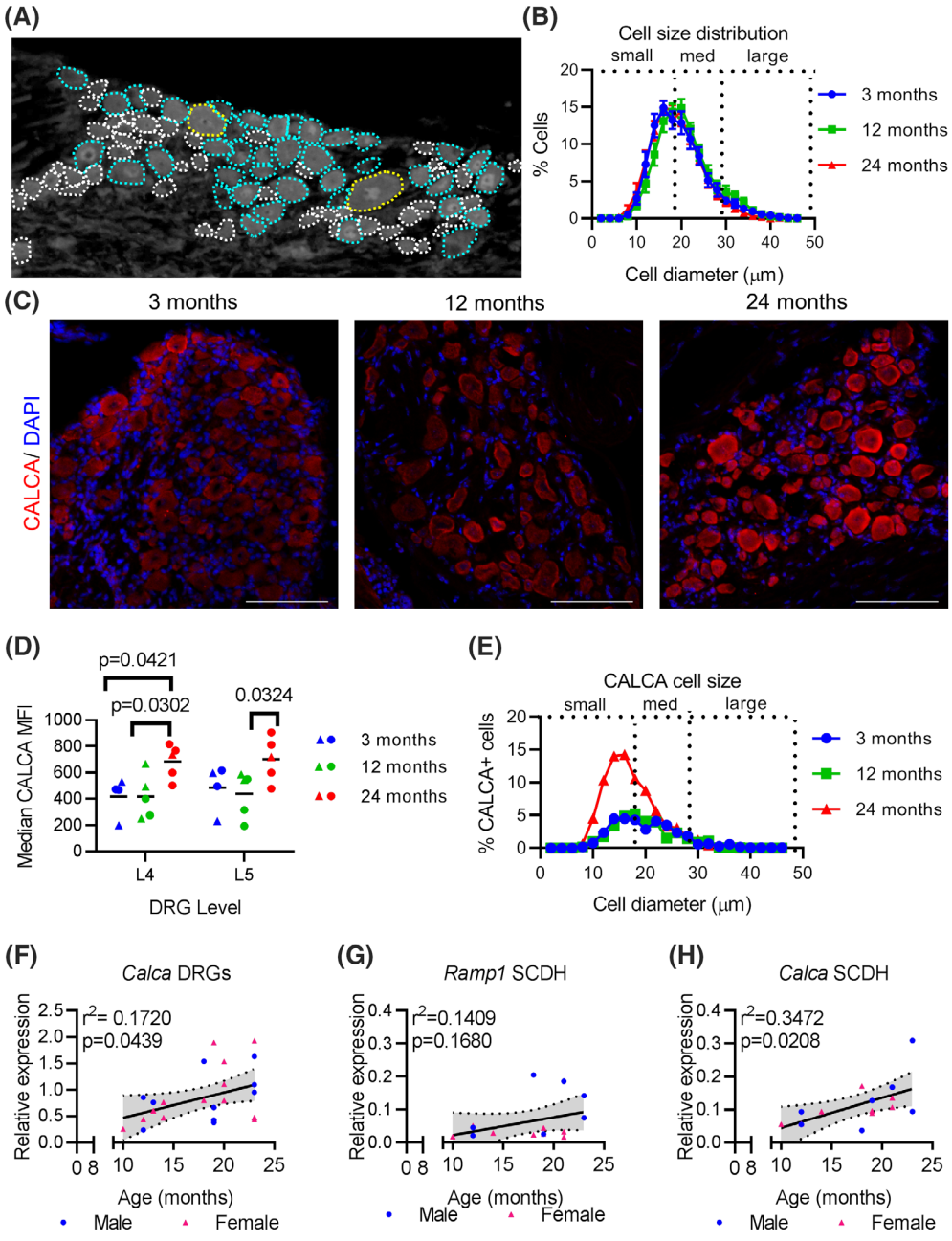

FIGURE 2 CALCA is transcriptionally regulated in the DRGs and spinal cord of aging mice. A, Depiction of a DRG with small (white), medium (teal), and large (yellow) diameter neurons outlined. B, Proportional distribution of DRG cells by diameter in mice 3, 12, and 24 months. Dotted lines demarcate approximate boundaries of small, medium, and large-diameter neurons. C, CALCA immunofluorescence in the L4/L5 DRGs of aging mice counterstained with DAPI. Scale bars, 100 μm. D, Median values of the mean fluorescent intensities (MFI) of cells within the L4 and L5 DRGs at indicated ages. Each point represents an individual animal. Black bars indicate group mean. E, Distribution of CALCA positive cells by cell size at indicated ages. F, qPCR analysis for Calca expression in L4-L6 DRGs normalized to Gapdh compared with age in a linear regression. G, qPCR analysis for Ramp1 expression in the lumbar spinal cord dorsal horn (SCDH) normalized to Gapdh compared with age. H, qPCR analysis for Calca expression in lumbar SCDH normalized to Gapdh compared with Linear regression line (solid black line) and 95% CI (dotted lines) are based on both sexes combined. Each point in a graph represents a single biological replicate

Following its release into the SCDH, CALCA acts on its receptors, Calcitonin receptor-like receptor in conjunction with receptor activity modifying protein 1 (RAMP1), which confers specificity. qPCR analysis show that the *Ramp1* mRNA expression is not correlated with age in the lumbar SCDH (Figure 2G). Further, *Ramp1* relative mRNA expression is comparable between 24 months and 12 months in the SCDH (Table 4). In contrast, relative mRNA expression of *Calca* within the lumbar SCDH is positively associated with age (^{1,13} F = 6.916, r^2 = 0.3472, *P* = .0208, n = 15) (Figure 2H), showing a substantial increase from 12 to 24 months (Table 4). These data indicate that CALCA protein production is elevated both peripherally and centrally with advanced age, and does not result in transcriptional regulation of its receptor *Ramp1* in the spinal cord.

Another neuropeptide involved in the transmission of nociception is TAC1, also known as Substance P. We conducted Western blot analysis to quantify TAC1 protein expression in the L4-6 DRGs with age (Figure 3A). Quantification of Western blot results showed a significant main effect of age on L4-6 DRG TAC1 protein content normalized to alpha-tubulin (^{4,15} F = 5.840, *P* = .0049, n = 5 per age cohort) (Figure 3B). Dunnett's post-hoc test revealed that 24-month-old L4-6 DRGs have significantly greater TAC1 protein than 12-month-old DRGs (^{15} F = 4.563, *P* = .0386). Alpha-tubulin protein intensity did not show a significant effect of age (*P* = .2190). Interestingly, the increased TAC1 protein is not due to changes at the transcriptional level as no significant change in the *Tac1* mRNA expression was observed in the L4-6 DRGs from 12 to 24 months (Figure 3C), and the relative mRNA expression of *Tac1* is comparable at each age group studied in the

DRGs (Table 4). The increased amount of TAC1 protein in DRGs prompted us to look at its receptor, Tachykinin receptor 1 (TACR1, also known as NK1), in the spinal cord. We found no correlation between *Tacr1* mRNA expression and age of mouse (Figure 3D), as its expression remains unchanged until 24 months of age (Table 4). Moreover, qPCR results show that *Tac1* mRNA expression is not regulated within the SCDH in aging mice (Figure 3E and Table 4). Results indicate that the increased TAC1 protein in aged DRGs does not affect the regulation of its receptor, TACR1, nor the local expression of *Tac1* at transcriptional level in the lumbar SCDH.

3.2 | Mediator of heat sensitivity, TRPV1, in DRGs is not affected by age, while mediator of cold sensitivity, TRPA1, increases variability with age

To assess the molecular regulation of heat and cold sensitivity, we characterized the expression of TRPV1, a heat-sensitive ion channel, and TRPA1, a cold-sensing ion channel, in the DRGs with age. Immunofluorescence analysis shows no change in TRPV1 protein intensity in either L4 or L5 DRGs with age (Figure 4A,B). Similarly, the distribution of TRPV1-positive cells showed comparable size distribution in all ages (Figure 4C). Previously we reported an increase in TRPA1 protein in the L4 and L5 DRGs by 24 months in mice.[15] Here we show that expression of this channel is regulated post-transcriptionally as mRNA expression of *Trpa1* is not significantly regulated with age in the L4-6 DRGs (Figure 4A). Comparing between ages, we found that the variability of *Trpa1* mRNA expression between cohorts was significantly different (Brown-Forsythe test $F^{2,21} = 7.436$, $P = .0036$, n = 24), necessitating the use of non-parametric testing. The Kruskal-Wallis test revealed that there was not a significant effect of age cohort on L4-6 DRG *Trpa1* mRNA expression (Table 4). Thus, while *Trpa1* expression becomes more variable with age, it is not significantly increased.

3.3 | DRGs respond to age-related inflammation but do not show transcriptional regulation of inflammatory mediators

Aging is a major risk factor for several degenerative diseases, including disc degeneration, and associated inflammation. To assess whether lumbar DRGs are responding to an increasingly inflamed environment, components of the NFκB pathway-a hallmark of inflammatory signaling-were investigated. qPCR analysis showed that mRNA expression of *Rela* is positively associated with aging in L4-6 DRGs ($F^{1,22} = 8.726$, $r^2 = 0.2840$, $P = .0073$, n = 24) (Figure 5A). In fact, the relative mRNA expression of *Rela* to *Gapdh* in 24-month-old L4-L6 DRGs is 1.97 times greater than that found in 12 month old L4-L6 DRGs (Table 4). Likewise, *Nfkb1* mRNA expression was also significantly associated with aging ($F^{1,22} = 16.11$, r2 = .04227, $P = .0006$, n = 24) (Figure 5B). One-way ANOVA revealed a significant effect of age ($F^{2,22} = 13.04$, $P = .0003$, n = 24) and post-hoc analysis demonstrated that 24-month-old DRGs have greater *Nfkb1* mRNA expression compared with both 12- and 18-month-old DRGs (Table 4). These data indicate there are substantial age-associated mRNA regulation of NFκB components indicating an enhanced response to inflammation.

We next determined whether inflammation driving NFκB expression in DRGs originates in DRG glial cells, which are known to contribute to inflammatory-driven pain,[31,32] or is derived from other aging tissues. Toward this, the expression of key inflammatory markers was assessed by qPCR in the L4-6 DRGs. No age-related changes in the mRNA expression of *Il1*, *Il6*, *Tnf*, *Gfap*, or *Cox2* were observed in the DRGs (n = 15 per assay) (Figure 5C-G and Table 4). These results indicate that the regulation of the mRNA expression of NFκB subunits is not mediated through local production of inflammatory mediators, but rather a response to inflammation originating in other tissues.

3.4 | Markers of peripheral nerve stress increases with age

To test whether increased neuronal stress with age, we did qPCR analysis to determine the expression of nerve stress markers *Atf3* and *Npy*. A linear regression of *Atf3* mRNA expression in L4-6 DRGs revealed a significant positive relationship with mouse age ($F^{1,22} = 9.082$, $r^2 = 0.2922$, $P = .0064$, n = 24) (Figure 6A). Post-hoc analysis revealed that 24-month-old L4-6 DRGs have significantly greater mRNA expression of *Atf3* than 12-month-old L4-6 DRGs (Table 4). While DRGs from aged mice show a trend for increasing *Npy* mRNA expression, the effect did not reach significance ($F^{1,12} = 4.511$, $r^2 = 0.2732$, $P = .0551$, n = 24) (Figure 6B), and the difference between 24- and 12-month-old DRGs did not reach significance ($P = .0526$, Table 4).

3.5 | Expression of neurotropic factor *Bdnf*, but not NGF, increases with age

One way in which tissues and nerves communicate following stress or damage is through the secretion, uptake, and production of neurotrophic factors including nerve growth factor (NGF) and brain derived neurotrophic factor (BDNF). We quantified NGF protein expression in the L4 and L5 DRGs by immunofluorescence and found comparable intensities between all age cohorts (Figure 7A,B). NGF-positive cells are also similarly distributed based on size across age cohorts and are found predominantly in the small to medium sized DRGs (Figure 7C). In contrast, *Bdnf* mRNA expression in L4-6 DRGs is significantly associated with mouse age ($F^{1,22} = 4.393$, $r^2 = 0.1801$, $P = .0497$, n = 24) (Figure 7D). L4-6 DRGs from 24-month-old mice have significantly greater *Bdnf* mRNA expression than 12-month-old mice (Table 4). To test whether the receptor for NGF, TRKA, was differentially expressed with age, we quantified immunoreactivity for TRKA protein in the L4 and L5 DRGs (Figure 7E,F). While the overall expression based on intensity of TRKA protein was comparable across groups,

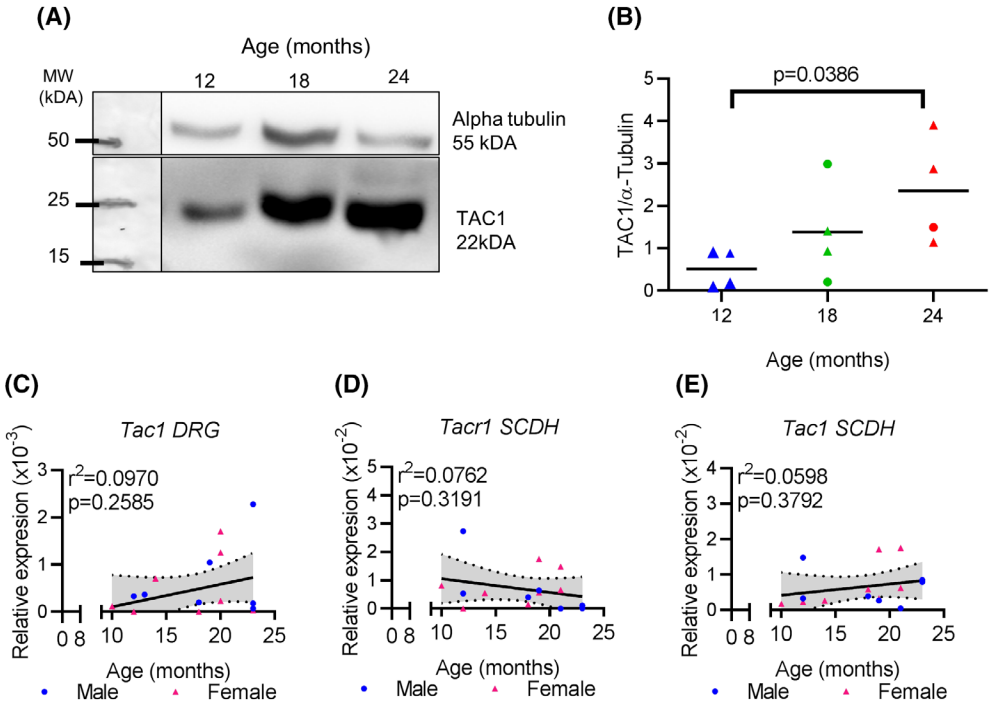

FIGURE 3 Aging DRGs have post-transcriptional increased expression of TAC1. A, Representative Western blot showing TAC1 and alpha-tubulin bands at indicated age. B, Quantification of four Western blots, using protein preparations from four different biological replicates, at indicated ages in the L4-6 DRGs showing TAC1 normalized to alpha-tubulin. C, qPCR analysis for Tac1 expression in L4-L6 DRGs normalized to Gapdh at indicated ages. D, qPCR analysis for Tacr1 expression in lumbar SCDH normalized to Gapdh at indicated ages. E, qPCR analysis for Tac1 expression in lumbar SCDH normalized to Gapdh at indicated ages. Linear regression (solid black line) and 95% CI (dotted lines) are based on both sexes combined. MW, molecular weight. kDA, kilodaltons. Each point in a graph represents a single biological replicate

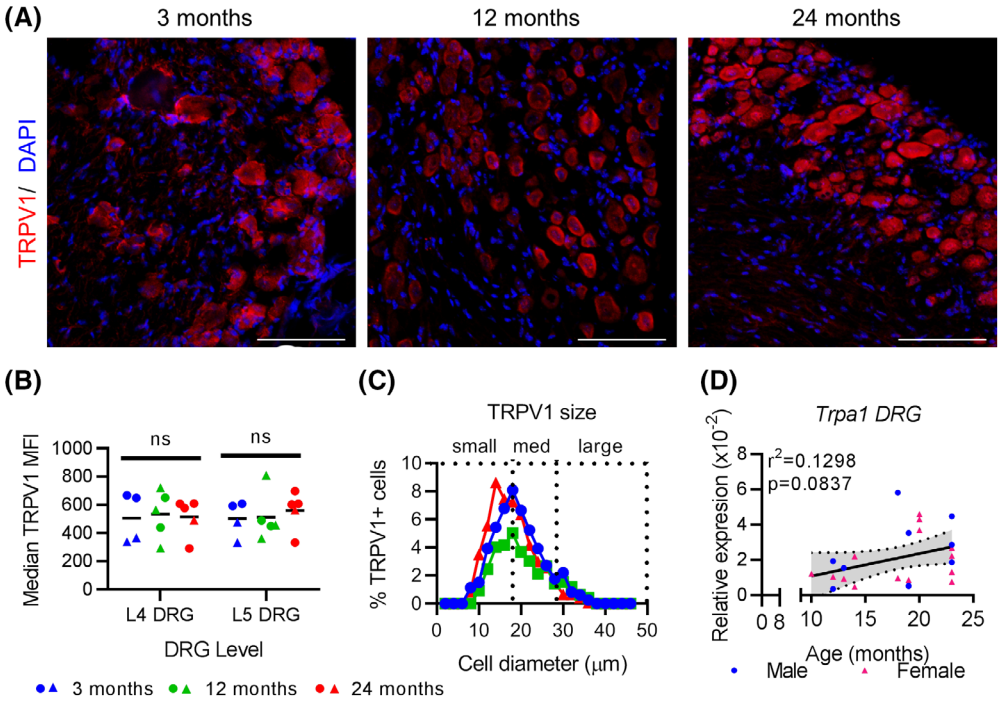

FIGURE 4 TRPV1 expression remains constant in L4-6 DRGs with age. A, TRPV1 immunofluorescence of the L4/L5 DRGs with DAPI counterstained nuclei at indicated ages. Scale bar, 100 μm. B, Median MFIs of cells within the L4 and L5 DRGs at indicated ages. Each point represents an individual animal. Black bars indicate group mean. ns, not significantly different. C, Distribution of TRPV1-positive cells by cell size at indicated ages. D, qPCR results for Trpa1 expression in L4-6 DRGs normalized to Gapdh at indicated ages. Linear regression (solid black line) and 95% CI (dotted lines) are based on both sexes combined. Each point in a graph represents a single biological replicate

TRKA-positive DRGs were more likely to be small diameter at 12 and 24 months compared with three-month-old mice (Figure 7G). These data suggest that the increase in *Bdnf* mRNA expression in aging DRGs is mediated through an NGF-independent mechanism.

4 | DISCUSSION

Here we show how the nociceptive signal transduction pathway progressively changes in mice as they age. We characterize these changes in distinct, but overlapping categories: nociceptive sensitization, nerve stress, inflammation, nerve growth, and thermal sensitivity. Importantly, these changes occur without a change in the cell size distribution. Instead, our results point to dynamic regulation at both the transcriptional and protein level. Specifically, aged DRGs have increased nociceptive neuropeptide expression, including TAC1 and CALCA protein; increased mRNA expression of NFκB subunits, *Nfkb1* and *Rela*; marker of stress, *Atf3*; and neurotropic factor, *Bdnf*. Importantly, these changes become substantial by 18 to 24 months in mice, which has been compared with 56 to 69 years in humans,[22] and coincides with worsening histopathological scores in the mouse lumbar discs.[18] However, mRNA levels of inflammatory markers, *Tnf*, *Il6*, *Il*b, *Cox2*, or *Gfap*, does not change with age in DRGs. Also, there are no age-related changes in the protein levels of TRKA/NGF or TRPV1 in the DRGs. Together these results point to a distinctive physiology for nociceptive transmission in aging mice.

Increased protein expression of the neuropeptides CALCA and TAC1 are one of the ways in which we found age affects DRGs at molecular level. Both neuropeptides have long established associations with the transmission and modulation of pain. Studies suggest CALCA does not produce acute pain itself, but rather its release causes lowered nociceptive thresholds, promoting central sensitization.[33,34] This is in line with behavioral data in mice showing increased sensitivity to acetone on the hind paw with age.[15] Similarly, muscle injury in aged rats induces long-lasting elevated CALCA expression in L4-L5 DRGs coinciding with protracted hind paw hyperalgesia.[35] This is in contrast to young rats that quickly recover from injury.[35] *Calca* mRNA expression positively correlated with aging in both DRGs and SCDH in this study. Increased CALCA at the protein level has been reported in the lumbar SCDH by 24 months of age in mice.[36]

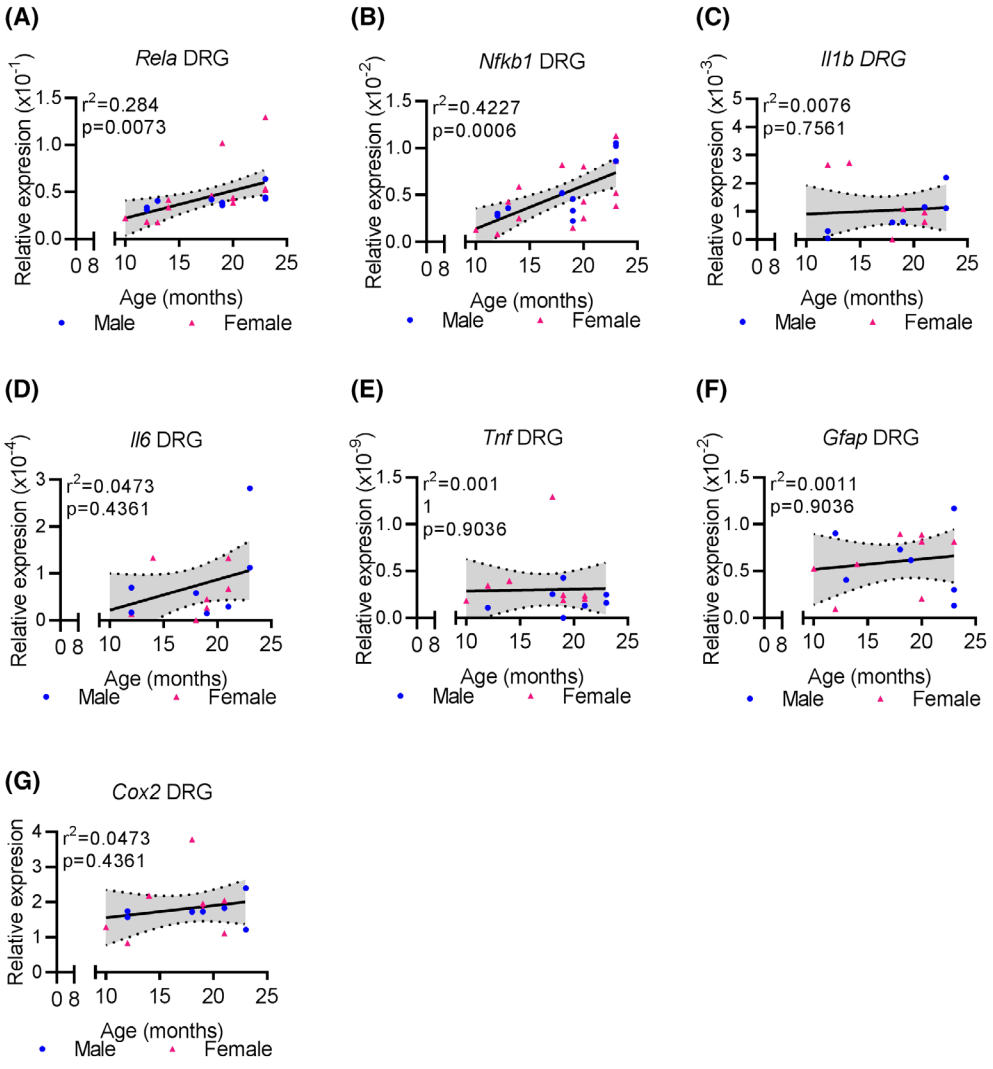

FIGURE 5 With age L4-6 DRGs increase expression of NFκB dimers, but not inflammatory mediators. A-G, qPCR analysis showing the expression of indicated gene expressed relative to Gapdh at indicated ages in both male and female mouse L4-6 DRGs. Linear regression (solid black line) and 95% CI (dotted lines) are based on both sexes combined. Each point in a graph represents a single biological replicate

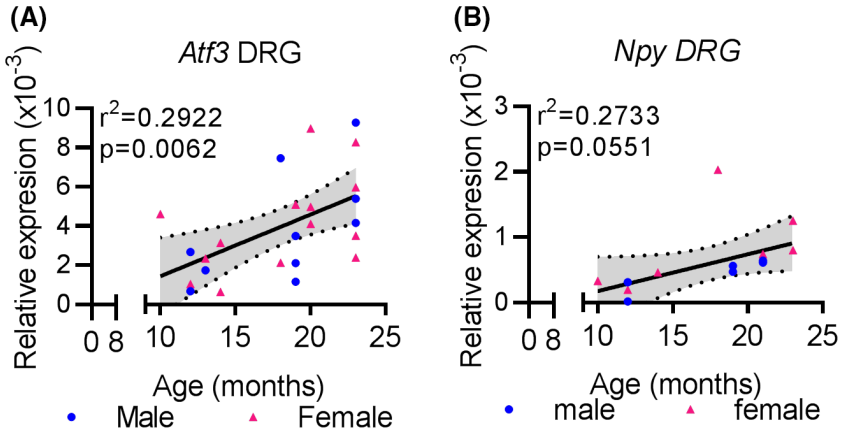

FIGURE 6 Increased signs of nerve damage with age in lumbar DRGs. A, qPCR analysis shows Atf3 expression in L4-L6 DRGs normalized to Gapdh at indicated ages. B, qPCR analysis for Npy expression in L4L6 DRGs normalized to Gapdh at indicated ages. Linear regression (solid black line) and 95% CI (dotted lines) are based on both sexes combined. Each point in a graph represents a single biological replicate

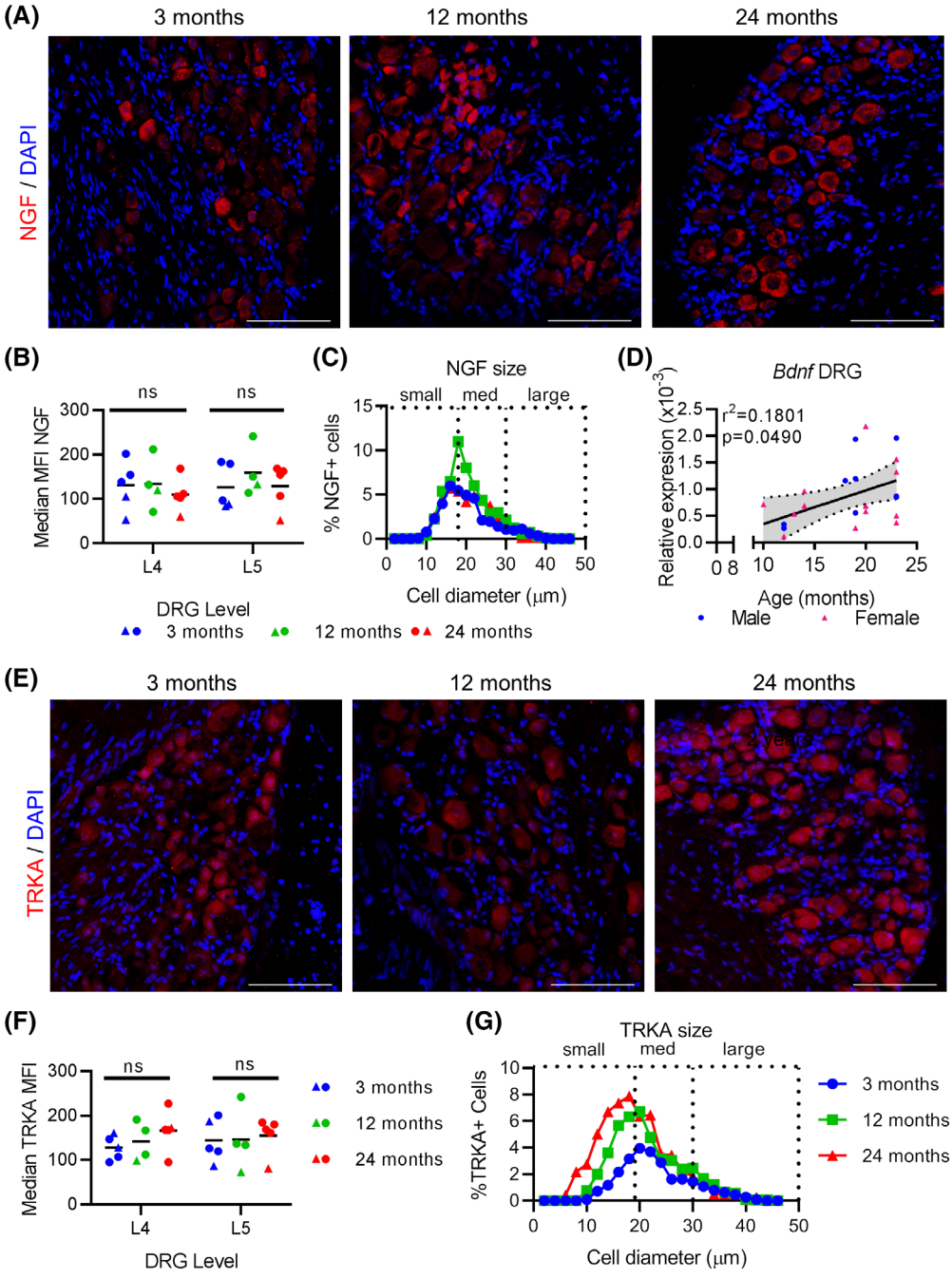

FIGURE 7 Bdnf expression is increased with age in L4-6 DRGs, but not NGF nor TrkA. A, Immunofluroescence of NGF in the L4/L5 DRGs at indicated ages with DAPI counterstained nuclei at indicated ages. Scale bar, 100 μm. B, Quantification of median MFIs of NGF in the L4/5 DRGs at indicated ages. Each point represents an individual animal. Black bars indicate group mean. ns, not significantly different. C, Relative distribution of NGF-positive cells based on cell diameter at indicated age groups. D, qPCR analysis for Bdnf expression in L4-L6 DRGs normalized to Gapdh at indicated ages. E, Immunofluorescence of TrkA in the L4/L5 DRGs at indicated ages with DAPI counterstained nuclei at indicated ages. Scale bar, 100 μm. Each point represents an individual animal. Black bars indicate group mean. F, Quantification of median MFIs of TrkA in the L4/5 DRGs at indicated ages. ns, not significantly different. G, Relative distribution of TrkA-positive cells based on cell diameter at indicated age groups. Each point in a graph represents a single biological replicate

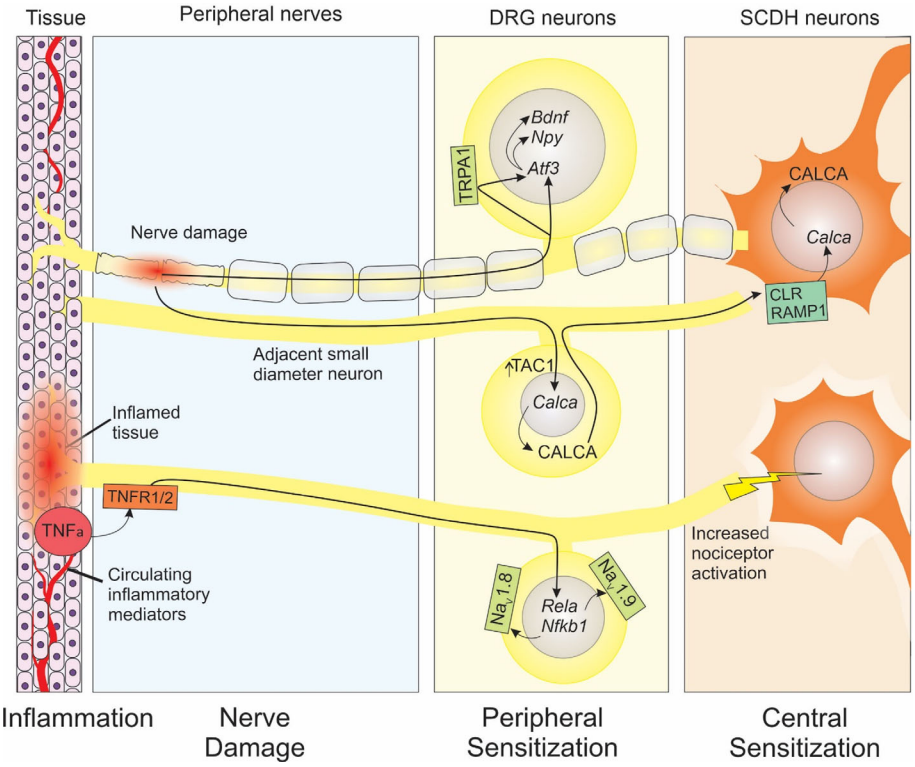

FIGURE 8 Model of response to aging in the mouse somatosensory nervous system. Damage to nerves and demyelination due to age-related degenerative diseases including intervertebral disc degeneration induces Atf3, possibly mediated by increased TRPA1 expression, which promotes expression of Npy and Bdnf. Nearby intact small diameter nerves respond to nerve damage by inducing Calca, resulting in increased CALCA expression which is transported to the SCDH which may induce further Calca expression in SCDH neurons, leading to central sensitization. Additionally, increased presence of TNFalpha in aging tissues or the circulatory system acts on its receptors, TNFR1/2, to induce NFκB pathway components, Rela and Nfkb1, which in turn increases expression of nociceptive sodium channels, NaV1.8 and NaV1.9. Higher sodium channel expression reduces thresholds and increases the stimulation of SCDH neurons

Interestingly, in this study we found no change in *Tac1* mRNA expression in either the DRGs or the SCDH with age despite observing an increase at the protein level. Previous reports have demonstrated that the rate of TAC1 protein synthesis and buildup in the nerve do not always align. For instance, in vitro synthesis of TAC1 in DRGs can be rapidly attenuated without a matched reduction in its protein concentration, indicating slow turnover.[37] Additionally, TAC1 protein accumulates in both the injured peripheral nerve and in the ganglion following in vitro DRG preparations, indicating there are two distinct pools of neuropeptide, one of which is axonally transported.[38] Indeed, it is known that 24-month-old mice have reduced sciatic nerve anterograde transport capacity and speed compared with 18-month-old mice.[39] Why transport is reduced in the sciatic nerve with age is not definitively clear; however, pathological distortions in the lumbar disc shape and height has been shown to displace nearby nerves, promoting nerve degeneration.[40] Whether the damage incurred is sufficient to impair neuropeptide transport remains to be tested.

While we did not find aged DRGs to have enhanced mRNA expression of inflammatory mediators, there may still be local inflammation, which could not be detected via qPCR. For instance, compromised mRNA stability of inflammatory mediators with age would cause expression levels to be underestimated. Assessing the inflammation at the protein level will also clarify the role of local inflammatory mediators in aging DRGs. Furthermore, isolating glia and macrophages within the DRGs for inflammatory mediator expression should be assessed in isolation to improve detection of subtle changes within cell subpopulations. We did however, observe increased age-associated mRNA expression of the NFκB pathway in DRGs. Activation of the NFκB pathway is a hallmark response to inflammation, most notably to TNFalpha. The NFκB dimers play a role in the chronic sensitization of DRG neurons via transcriptional[41-45] and post-transcriptional[46] regulation of excitatory channels. This phenomenon has been described in models of nerve injury,[45] diabetic neuropathy,[44] and post-surgical pain,[42] suggesting multiple chronic pain conditions may be mediated by NFκB induction. This is particularly relevant in the context of age-related degenerative disorders. Degenerated lumbar discs are a known source of inflammatory mediators including TNFalpha, IL1alpha, IL1beta, and IL6,[47] and the concentration of these mediators in the serum is directly associated with lumbar pain in humans.[48] In mouse models, TNFalpha induces axonal growth into degenerated discs.[49] Furthermore, lumbar disc inflammation has been shown to promote CALCA-positive nerve ingrowth into the affected discs, providing a putative mechanism for discogenic pain.[50] In addition, we previously showed that 24-month-old mice with disc degeneration have increased nociceptive sodium channels, $Na_V1.8$ and $Na_V1.9$, in the L4/5 DRGs,[15] which have been shown to be a downstream target of NFκB in pain conditions.[42,44,45] This suggests the possibility that secretion of TNFalpha by aging tissues, such as the lumbar discs, induces expression of painful mediators, including Na_Vs and CALCA, in DRGs via NFκB pathways, promoting pain signaling (shown in Figure 8).

An important finding in our study showed an increase in *Atf3*, *Calca*, and *Bdnf* mRNA in aging DRGs. We have previously demonstrated that in addition to developing cold allodynia in the hind paws, old mice have greater protein expression of the cold-sensing ion channel, TRPA1, in L4/5 DRGs.[15] TRPA1 has also been implicated in mediating ATF3 induction following low doses of formalin and mustard oil.[51] Importantly, this mediation occurs for low level nerve damage,

similar to what we observe in aged animals, and was not required for the induction of ATF3 protein when high level of exogenous noxious stimuli were applied.[51] Our analyses cannot point to causal relationship between *Trpa1* and *Atf3* mRNA; however, our findings are in line with experimental models showing TRPA1-mediated ATF3 induction during low level nerve stress exposure (Figure 8).

While all assays were performed on the same set of biological replicates, it is important to note that these assays cannot determine whether the same cells within the DRGs are expressing these markers. Neuropathic pain is thought in part to be mediated by the sensitization of the surrounding intact axons and aberrant nerve sprouting, referred to as the "intact nociceptor hypothesis" (reviewed in Reference52). Thus, elevated *Calca* mRNA and CALCA protein with age in DRGs may indicate sensitization of intact nociceptors in response to nearby damaged neurons (Figure 8). In contrast to CALCA which is predominantly in intact neurons,[53] BDNF does appear in ATF3-positive neurons.[54] Importantly, ATF3/BDNF double-labelling is limited to nerve injuries which produce neuropathic pain, and does not occur in innocuous nerve injuries.[54] BDNF has also been shown to induce late long-term potentials in C-fiber-evoked field potentials in the SCDH by inducing protein synthesis, indicating that BDNF release from nociceptors can induce central sensitization.[55] Our results do not point to a specific cause for the nerve stress response; however, nerve crush from facet joints or disc herniation are age-related phenomena, which could produce a stress response,[56,57] and needs further validation in preclinical models of disc degeneration.

Future research should also investigate the more rostral DRG levels. Importantly, our results show changes specific to the L4-L6 as they are proximal to the caudal lumbar IVDs; however, the L5/L6 IVD alone is innervated from neurons from T13-L6 DRGs, making them candidates for disc-driven changes with age.[58-60] Though our research was motivated by our findings in the lumbar disc with age, the results presented here cannot relate to a specific source. Indeed, the changes observed may be the result of increased circulating pro-inflammatory mediators,[61] is due to various age-related pathologies including degeneration in the knees,[62] muscular atrophy,[63] or other heterogeneous aging phenomenon. Further, while our findings include both male and female mice, the small sample size of each precludes analysis of sex-differences in our data. We did not anticipate sex differences as our earlier well-powered models of aging showed comparable behavioral and molecular profiles in male and female mice after accounting for weight differences.[15] However, behavioral studies are increasingly observing reliable sex differences in both pain behaviors and biology (reviewed here[64]), and how these differences interact with age is of interest to the both the pain and aging community.

With the global aging population, the burden of diseases affecting the elderly, such as, cancers, diabetes, and musculoskeletal disorders, continues to rise.[65] As a result, developing treatment for those affected by diabetic and chemotherapy-induced neuropathies, rheumatoid and osteoarthritis, and low back and neck pain is becoming more critical. Key to optimizing assessment and treatment plans for chronic pain in the elderly will depend on characterizing how their physiology presents a unique environment for the somatosensory system. Unfortunately, many preclinical models use young and otherwise healthy animals to understand the initiation, progression, and treatment of these disorders, which may ultimately have limited translational potential to aging populations. We show here that aged mice are more likely to have signs of sensitization at the peripheral and central level. Further, the cells which make up the DRG are in a state of elevated response to inflammation, which itself may uniquely contribute to nociception by sensitizing neurons via the NFκB pathway. These changes have two important features: they are modest in size and occur gradually with age. As such, they identify a slowly shifting baseline in the sensory nervous system that becomes progressively more painful with age.

ACKNOWLEDGMENTS

Research reported in this publication was supported by the National Institute of Arthritis and Musculoskeletal and Skin Diseases of the National Institutes of Health under Award Number R01AR065530 awarded to CLD. The content is solely the responsibility of the authors and does not necessarily represent the official views of the National Institutes of Health. The research was also supported by the research endowment from Starr Chair in Tissue Engineering made to CLD, and research grants from Gerstner Family Foundation and S & L Marx Foundation made to CLD.

CONFLICT OF INTEREST

The authors declare no potential conflict of interest.

AUTHOR CONTRIBUTION

CLD conceived and designed the study, supervised the project and acquired funding. KV performed experiments and collected data. CPGD provided technical assistance. KV performed the data analysis. CLD, KV, and TJA interpreted the data. KV and CLD wrote the manuscript and prepared the figures. All authors reviewed the manuscript and gave their final approval.

ORCID

Chitra Lekha Dahia https://orcid.org/0000-0003-3683-9791

REFERENCES

1. Fayaz A, Croft P, Langford RM, Donaldson LJ, Jones GT. Prevalence of chronic pain in the UK: a systematic review and meta-analysis of population studies. *BMJ Open*. 2016;*6*(6):e010364.
2. National Population Projections Tables. United States Census Bureau. 2018
3. Gagliese L. Pain and aging: the emergence of a new subfield of pain research. *J Pain*. 2009;*10*:343-353.
4. Thomas PK, King RHM, Sharma AK. Changes with age in the peripheral nerves of the rat—an ultrastructural study. *Acta Neuropathol*. 1980;*52*:1-6.
5. Grover-Johnson N, Spencer PS. Peripheral nerve abnormalities in aging rats. *J Neuropathol Exp Neurol*. 1981;*40*:155-165.
6. Cole LJ, Farrell MJ, Gibson SJ, Egan GF. Age-related differences in pain sensitivity and regional brain activity evoked by noxious pressure. *Neurobiol Aging*. 2010;*31*:494-503.
7. Gerli R, Monti D, Bistoni O, et al. Chemokines, sTNF-Rs and sCD30 serum levels in healthy aged people and centenarians. *Mech Ageing Dev*. 2000;*121*(1-3):37–46.

8. Ballou SP, Lozanski GB, Hodder S, et al. Quantitative and qualitative alterations of acute-phase proteins in healthy elderly persons. *Age Ageing*. 1996;*25*:224-230.
9. Grönblad M, Weinstein JN, Santavirta S. Immunohistochemical observations on spinal tissue innervation: a review of hypothetical mechanisms of back pain. *Acta Orthop*. 1991;*62*:614-622.
10. Coppes MH, Marani E, Thomeer RT, Groen GJ. Innervation of "painful" lumbar discs. *Spine*. 1976;*22*(20):2342-2349.
11. Nikodemova M, Small AL, Kimyon RS, Watters JJ. Age-dependent differences in microglial responses to systemic inflammation are evident as early as middle age. *Physiol Genomics*. 2016;*48*:336-344.
12. Kinsey SG, Bailey MT, Sheridan JF, Padgett DA. The inflammatory response to social defeat is increased in older mice. *Physiol Behav*. 2008;*93*:628-636.
13. Jimenez-Andrade JM, Mantyh PW. Sensory and sympathetic nerve fibers undergo sprouting and neuroma formation in the painful arthritic joint of geriatric mice. *Arthritis Res Ther*. 2012;*14*:R101.
14. Ray MA, Johnston NA, Verhulst S, Trammell RA, Toth LA. Identification of markers for imminent death in mice used in longevity and aging research. *J Am Assoc Lab Anim Sci*. 2010;*49*(3):282–288.
15. Vincent K, Mohanty S, Pinelli R, et al. Aging of mouse intervertebral disc and association with back pain. *Bone*. 2019;*123*(Jun):246–259.
16. Millecamps M, Shi XQ, Piltonen M, et al. The geriatric pain experience in mice: intact cutaneous thresholds but altered responses to tonic and chronic pain. *Neurobiol Aging*. 2019;*89*:1–11.
17. Winkler T, Mahoney EJ, Sinner D, Wylie CC, Dahia CL. Wnt signaling activates Shh signaling in early postnatal intervertebral discs, and re-activates Shh signaling in old discs in the mouse. *PLoS One*. 2014;*9*(6):e98444.
18. Mohanty S, Pinelli R, Pricop P, Albert TJ, Dahia CL. Chondrocyte-like nested cells in the aged intervertebral disc are late-stage nucleus pulposus cells. *Aging Cell*. 2019;*18*(5):e13006.
19. Shortland PJ, Krzyzanowska A, Priestley JV, Averill S. ATF3 expression in L4 dorsal root ganglion neurons after L5 spinal nerve transection. *Artic Eur J Neurosci*. 2006;*23*(2):365–373.
20. Averill S, Michael GJ, Shortland PJ, et al. NGF and GDNF ameliorate the increase in ATF3 expression which occurs in dorsal root ganglion cells in response to peripheral nerve injury. *J Eur Neurosci*. 2004;*19*:1437-1445.
21. Tsujino H, Kondo E, Fukuoka T, et al. Activating transcription factor 3 (ATF3) induction by axotomy in sensory and motoneurons: a novel neuronal marker of nerve injury. *Mol Cell Neurosci*. 2000;*15*(2):170-182.
22. Hagan C. When are mice considered old? *The Jackson Laboratory*. 2017. https://www.jax.org/news-and-insights/jax-blog/2017/november/when-are-mice-considered-old.
23. Malin SA, Davis BM, Molliver DC. Production of dissociated sensory neuron cultures and considerations for their use in studying neuronal function and plasticity. *Nat Protoc*. 2007;*2*(1):152-160.
24. Keating C, Nocchi L, Yu Y, Donovan J, Grundy D. Ageing and gastrointestinal sensory function: altered colonic mechanosensory and chemosensory function in the aged mouse. *J Physiol*. 2016;*594*(16):4549-4564.
25. Bangaru MLY, Park F, Hudmon A, McCallum JB, Hogan QH. Quantification of gene expression after painful nerve injury: validation of optimal reference genes. *J Mol Neurosci*. 2012;*46*:497-504.
26. Dahia CL, Mahoney E, Wylie C. Shh signaling from the nucleus pulposus is required for the postnatal growth and differentiation of the mouse intervertebral disc. *PLoS One*. 2012;*7*(4):e35944.
27. Mincheva-Tasheva S, Obis E, Tamarit J, Ros J. Apoptotic cell death and altered calcium homeostasis caused by frataxin depletion in dorsal root ganglia neurons can be prevented by BH4 domain of Bcl-xL protein. *Hum Mol Genet*. 2014;*23*:1829-1841.
28. D'Agostino G, La Rana G, Russo R, et al. Central administration of palmitoylethanolamide reduces hyperalgesia in mice via inhibition of NF-κB nuclear signalling in dorsal root ganglia. *Eur J Pharmacol*. 2009;*613*:54-59.
29. Lawson SN. The postnatal development of large light and small dark neurons in mouse dorsal root ganglia: a statistical analysis of cell numbers and size. *J Neurocytol*. 1979;*8*:275-294.
30. Lawson SN. Neuropeptides in morphologically and functionally identified primary afferent neurons in dorsal root ganglia: substance P, CGRP and somatostatin. In: Nyberg F, Hari Shanker Sharma Z, eds. *Neuropeptides in the Spinal Cord. Wiesenfeld-Hallin*. Amsterdam - Lausanne - New York - Oxford - Shannon -Tokyo: Elsevier Science; 1995:421.
31. Wagner R, Myers RR. Endoneurial injection of TNF-α produces neuropathic pain behaviors. *Neuroreport*. 1996;*7*:2897-2902.
32. Wagner R, Myers RR. Schwann cells produce tumor necrosis factor alpha: expression in injured and non-injured nerves. *Neuroscience*. 1996;*73*:625-629.
33. Nakamura-Craig M, Gill BK. Effect of neurokinin a, substance P and calcitonin gene related peptide in peripheral hyperalgesia in the rat paw. *Neurosci Lett*. 1991;*124*:49-51.
34. Bird GC, Han JS, Fu Y, Adwanikar H, Willis WD, Neugebauer V. Pain-related synaptic plasticity in spinal dorsal horn neurons: role of CGRP. *Mol Pain*. 2006;*2*. https://doi.org/10.1186/1744-8069-2-31.
35. Johnson C, Miller GR, Baker BA, et al. Changes in the expression of calcitonin gene-related peptide after exposure to injurious stretch-shortening contractions. *Exp Gerontol*. 2016;*79*:1-7.
36. Miyagi M, Millecamps M, Danco AT, Ohtori S, Takahashi K, Stone LS. ISSLS Prize winner: Increased innervation and sensory nervous system plasticity in a mouse model of low back pain due to intervertebral disc degeneration. *Spine*. 2014;*39*(17):1345-1354.
37. Nielsch U, Bisby MA, Keen P. Effect of cutting or crushing the rat sciatic nerve on synthesis of substance P by isolated L5 dorsal root ganglia. *Neuropeptides*. 1987;*10*(2):137-145.
38. Harmar A, Keen P. Synthesis, and central and peripheral axonal transport of substance P in a dorsal root ganglion-nerve preparation in vitro. *Brain Res*. 1982;*231*(2):379-385.
39. Milde S, Adalbert R, Elaman MH, Coleman MP. Axonal transport declines with age in two distinct phases separated by a period of relative stability. *Neurobiol Aging*. 2015;*36*:971-981.
40. Harris RI, Macnab I. Structural changes in the lumbar intervertebral discs; their relationship to low back pain and sciatica. *J Bone Joint Surg Br*. 1954;*36-B*:304-322.
41. Tamura R, Nemoto T, Maruta T, et al. Up-regulation of NaV1.7 sodium channels expression by tumor necrosis factor-α in cultured bovine adrenal chromaffin cells and rat dorsal root ganglion neurons. *Anesth Analg*. 2014;*118*(2):318-324.
42. Li Z, Li Y, Cao J, et al. Membrane protein Nav1.7 contributes to the persistent post-surgical pain regulated by p-p65 in dorsal root ganglion (DRG) of SMIR rats model. *BMC Anesthesiol*. 2017;*17*(1):150.
43. Zhao R, Pei GX, Cong R, Zhang H, Zang CW, Tian T. PKC-NF-κB are involved in CCL2-induced Nav1.8 expression and channel function in dorsal root ganglion neurons. *Biosci Rep*. 2014;*34*(3):237-245.
44. Huang Y, Zang Y, Zhou L, Gui W, Liu X, Zhong Y. The role of TNF-alpha/NF-kappa B pathway on the up-regulation of voltage-gated sodium channel Nav1.7 in DRG neurons of rats with diabetic neuropathy. *Neurochem Int*. 2014;*75*:112-119.
45. He XH, Zang Y, Chen X, et al. TNF-α contributes to up-regulation of Nav1.3 and Nav1.8 in DRG neurons following motor fiber injury. *Pain*. 2010 Nov;*151*(2):266-279.
46. Xie M-X, Zhang X-L, Xu J, Pang R-P, Ma K, Liu X-G. Nuclear factor-kappaB gates Na v 1.7 channels in DRG neurons via protein-protein interaction. *IScience*. 2019;*19*:623-633. https://doi.org/10.1016/j.isci.
47. Takahashi H, Suguro T, Okazima Y, Motegi M, Okada Y, Kakiuchi T. Inflammatory cytokines in the herniated disc of the lumbar spine. *Spine*. 1996;*12*(104):20141191.

48. Wang K, Bao JP, Yang S, et al. A cohort study comparing the serum levels of pro- or anti-inflammatory cytokines in patients with lumbar radicular pain and healthy subjects. *Eur Spine J*. 2016;*25*(5):1428–1434.
49. Hayashi S, Taira A, Inoue G, et al. TNF-alpha in nucleus pulposus induces sensory nerve growth a study of the mechanism of discogenic low back pain using tnf-alpha-deficient mice. *Spine*. 2008;*33*(14):1542–1546.
50. Aoki Y, Ohtori S, Ino H, et al. Disc inflammation potentially promotes axonal regeneration of dorsal root ganglion neurons innervating lumbar intervertebral disc in rats. *Spine*. 2004;*29*(23):2621–2626.
51. Bráz JM, Basbaum AI. Differential ATF3 expression in dorsal root ganglion neurons reveals the profile of primary afferents engaged by diverse noxious chemical stimuli. *Pain*. 2010;*150*:290-301.
52. Campbell JN. Nerve lesions and the generation of pain. *Muscle Nerve*. 2001;*24*:1261-1273.
53. Li XQ, Verge VMK, Johnston JM, Zochodne DW. CGRP peptide and regenerating sensory axons. *J Neuropathol Exp Neurol*. 2004;*63*:1092-1103.
54. Zhou LJH, Ren WJ, Zhong Y, et al. Limited BDNF contributes to the failure of injury to skin afferents to produce a neuropathic pain condition. *Pain*. 2010;*148*:148-157.
55. Zhou LJ, Zhong Y, Ren WJ, Li YY, Zhang T, Liu XG. BDNF induces late-phase LTP of C-fiber evoked field potentials in rat spinal dorsal horn. *Exp Neurol*. 2008;*212*:507-514.
56. Inoue G, Ohtori S, Aoki Y, et al. Exposure of the nucleus pulposus to the outside of the anulus fibrosus induces nerve injury and regeneration of the afferent fibers innervating the lumbar intervertebral discs in rats. *Spine*. 2006;*31*(13):1433-1438.
57. Aoki Y, Ohtori S, Takahashi K, et al. Innervation of the lumbar intervertebral disc by nerve growth factor-dependent neurons related to inflammatory pain. *Spine*. 2004;*29*(10):1077-1081.
58. Ohtori S, Takahashi Y, Takahashi K, et al. Sensory innervation of the dorsal portion of the lumbar intervertebral disc in rats. *Spine*. 1999;*24*(22):2295-2299.
59. Ohtori S, Takahashi K, Chiba T, Yamagata M, Sameda H, Moriya H. Brain-derived neurotrophic factor and vanilloid receptor subtype 1 immunoreactive sensory DRG neurons innervating the lumbar facet joints in rats. *Auton Neurosci*. 2001;*94*(132):132-135.
60. Aoki Y, Takahashi Y, Takahashi K, et al. Sensory innervation of the portion of the lumbar intervertebral disc in rats. *Spine*. 2004;*4*(3):275-280.
61. Michaud M, Balardy L, Moulis G, et al. Proinflammatory cytokines, aging, and age-related diseases. *J Am Med Dir Assoc*. 2013;*14*:877-882.
62. Salo PT, Tatton WG. Age-related loss of knee joint afferents in mice. *J Neurosci Res*. 1993;*35*:664-677.
63. Chai RJ, Vukovic J, Dunlop S, Grounds MD, Shavlakadze T. Striking denervation of neuromuscular junctions without lumbar motoneuron loss in geriatric mouse muscle. *PLoS One*. 2011;*6*:e28090.
64. Greenspan JD, Craft RM, LeResche L, et al. Studying sex and gender differences in pain and analgesia: a consensus report. *Pain*. 2007;*132*:S26-S45.
65. GBD 2015 DALYs and HALE Collaborators G 2015 Daly and H, GBD 2015 DALYs and HALE Collaborators NJ, Arora M, Barber RM, Bhutta ZA, Brown J, et al. Global, regional, and national disability-adjusted life-years (DALYs) for 315 diseases and injuries and healthy life expectancy (HALE), 1990–2015: a systematic analysis for the global burden of disease study 2015. *Lancet*. 2016;*388*(10053):1603-1658.
66. Meyer R, Hatada EN, Hohmann HP, et al. Cloning of the DNA-binding subunit of human nuclear factor κB: the level of its mRNA is strongly regulated by phorbol ester or tumor necrosis factor α. *Proc Natl Acad Sci*. 1991;*88*:966-970.
67. Nolan GP, Ghosh S, Liou HC, Tempst P, Baltimore D. DNA binding and IκB inhibition of the cloned p65 subunit of NF-κB, a rel-related polypeptide. *Cell*. 1991;*64*(5):961-969.
68. Sen R, Baltimore D. Multiple nuclear factors interact with the immunoglobulin enhancer sequences. *Cell*. 1986;*46*(5):705-716.
69. Siemionow K, Klimczak A, Brzezicki G, Siemionow M, RF ML. The effects of inflammation on glial Fibrillary acidic protein expression in satellite cells of the dorsal root ganglion. *Spine*. 2009;*34*(16):1631-1637.
70. Gauldie J, Richards C, Harnish D, Lansdorp P, Baumann H. Interferon beta 2/B-cell stimulatory factor type 2 shares identity with monocyte-derived hepatocyte-stimulating factor and regulates the major acute phase protein response in liver cells. *Proc Natl Acad Sci*. 1987;*84*(20):7251-7255.
71. Beloeil H, Ji R-R, Berde CB. Effects of bupivacaine and Tetrodotoxin on carrageenan-induced hind paw inflammation in rats (part 2). *Anesthesiology*. 2006;*105*(1):139-145.
72. Junger H, Sorkin LS. Nociceptive and inflammatory effects of subcutaneous TNFα. *Pain*. 2000;*85*:145-151.
73. Ichitani Y, Shi T, Haeggstrom JZ, Samuelsson B, Hökfelt T. Increased levels of cyclooxygenase-2 mRNA in the rat spinal cord after peripheral inflammation: an in situ hybridization study. *Neuroreport*. 1997;*8*:2949-2952.
74. Amaya F, Samad TA, Barrett L, Broom DC, Woolf CJ. Periganglionic inflammation elicits a distally radiating pain hypersensitivity by promoting COX-2 induction in the dorsal root ganglion. *Pain*. 2009;*142*(1):59-67.
75. McCoy ES, Taylor-Blake B, Zylka MJ. CGRPα-expressing sensory neurons respond to stimuli that evoke sensations of pain and itch. *PLoS One*. 2012;7:e36355.
76. Cuello AC. Peptides as neuromodulators in primary sensory neurons. *Neuropharmacology*. 1987;*26*:971-979.
77. Ribeiro-da-Silva A, Hökfelt T. Neuroanatomical localisation of substance P in the CNS and sensory neurons. *Neuropeptides*. 2000;*34*:256-271.
78. Cottrell GS, Roosterman D, Marvizon JC, et al. Localization of calcitonin receptor-like receptor and receptor activity modifying protein 1 in enteric neurons, dorsal root ganglia, and the spinal cord of the rat. *J Comp Neurol*. 2005;*490*:239-255.
79. Iyengar S, Ossipov MH, Johnson KW. The role of calcitonin gene-related peptide in peripheral and central pain mechanisms including migraine. *Pain*. 2017;*158*:543-559.
80. Nichols ML, Allen BJ, Rogers SD, et al. Transmission of chronic nociception by spinal neurons expressing the substance P receptor. *Science*. 1999;*286*:1558-1561.
81. Obata K, Katsura H, Mizushima T, et al. TRPA1 induced in sensory neurons contributes to cold hyperalgesia after inflammation and nerve injury. *J Clin Invest*. 2005;*115*(9):2393-2401.
82. Wakisaka S, Kajander KC, Bennett GJ. Increased neuropeptide Y (NPY)-like immunoreactivity in rat sensory neurons following peripheral axotomy. *Neurosci Lett*. 1991;*124*(2):200–203.
83. Abdulla FA, Smith PA. Nerve injury increases an excitatory action of neuropeptide Y and Y2- agonists on dorsal root ganglion neurons. *Neuroscience*. 1999;*89*:43-60.
84. Obata K, Noguchi K. BDNF in sensory neurons and chronic pain. *Neurosci Res*. 2006;*55*(1):1-10.

How to cite this article: Vincent K, Dona CPG, Albert TJ, Dahia CL. Age-related molecular changes in the lumbar dorsal root ganglia of mice: Signs of sensitization, and inflammatory response. *JOR Spine*. 2020;3:e1124. https://doi.org/10.1002/jsp2.1124